Magnetic properties of the field-induced ferromagnetic state in MnSi

2009 J. Phys.: Condens. Matter 21 296003

(http://iopscience.iop.org/0953-8984/21/29/296003)

J. Phys.: Condens. Matter **21** (2009) 296003 (5pp) doi:10.1088/0953-8984/21/29/296003

Magnetic properties of the field-induced ferromagnetic state in MnSi

M K Chattopadhyay, Parul Arora and S B Roy

Magnetic and Superconducting Materials Section, Raja Ramanna Centre for Advanced Technology, Indore 452 013, India

Received 6 May 2009
Published 3 July 2009
Online at stacks.iop.org/JPhysCM/21/296003

Abstract

We present results of dc magnetization measurements focusing on the magnetic properties of the field-induced ferromagnetic state in MnSi. The temperature dependence of saturation magnetization in this ferromagnetic state exhibits the signatures of both spin wave excitations and itinerant electron ferromagnetism. The Arrott plots obtained from the isothermal field dependence of magnetization, however, are found to be distinctly nonlinear and hence cannot be explained within a simple framework of itinerant electron magnetism.

(Some figures in this article are in colour only in the electronic version)

1. Introduction

MnSi is a weak itinerant helimagnet [1] with an ordering temperature just below 30 K [2]. The compound has a B20-type crystal structure where the helical spin structure appears due to the presence of a Dzyaloshinski–Moriya interaction along with the ferromagnetic exchange interaction [3]. Application of a magnetic field below the ordering temperature leads to successive field-induced phase transitions starting from the helimagnetic phase (in zero and low fields) to a state with conical spin structure around 650 Oe, and then with further increase in the field to a ferromagnetic state above 6 kOe [1]. The lower field-induced magnetic transition is of first-order nature, and it shows the signatures of kinetic arrest in the field-decreasing cycle [4]. The zero and low field thermodynamic and transport properties of MnSi have drawn much attention in recent times in connection with quantum critical phenomenon and non-Fermi liquid behaviour [5–7]. In addition the nature of the magnetic transition in MnSi under ambient condition and external pressure has also been a subject of considerable attention [8–15]. In comparison there is not much information available on the magnetic properties of the field-induced ferromagnetic state of MnSi.

In the present work the magnetic properties of the higher field ferromagnetic phase of MnSi is investigated in detail through dc magnetization measurements. The temperature dependence of high field magnetization shows signatures indicating the role of both spin wave excitations and Stoner band excitations related to itinerant electron ferromagnetism. The nature of the magnetic state is investigated further through the study of Arrott plots.

2. Experimental details

The polycrystalline MnSi sample used in the present study was synthesized by arc-melting elemental Mn and Si in an argon atmosphere. The resulting button was flipped and re-melted several times to ensure sample homogeneity. The sample was then annealed at 800 °C for 7 d, and was subsequently characterized with x-ray diffraction (XRD), optical metallography and energy dispersive x-ray analysis (EDX). The XRD results confirm that the present MnSi sample has formed in the B20-cubic crystal structure. All the peaks in the XRD pattern are consistent with the B20-cubic structure. Within the experimental resolution, no other impurity peak was visible. From the optical metallography study the average grain size was estimated to be above 100 μm and with very narrow grain boundaries. EDX measurements at five different points in a test sample of 2 mm $\times$ 1 mm surface area showed a variation of the Mn:Si ratio between 1.03 and 0.96.

The same sample has been used for previous studies [4, 15]. The results of low field magnetization and specific heat measurements reported in these studies further ensures the good quality of the sample. Magnetization (M) measurements were performed on the MnSi sample as a function of temperature (T) and magnetic field (H) in a vibrating sample magnetometer (VSM, Quantum Design).

3. Results and discussion

Figures 1(a) and (b) show the temperature dependence of magnetization of MnSi in 100 Oe and 10 kOe magnetic

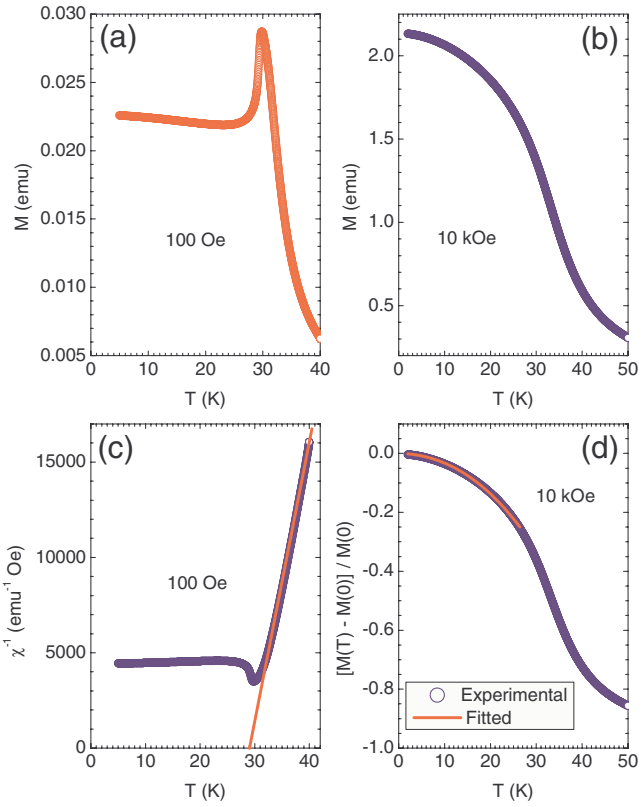

Figure 1. Temperature dependence of magnetization of MnSi. (a) Measurements done while warming up the sample in 100 Oe magnetic field, after cooling the sample in zero field (see [4] as well). (b) Magnetization measured while warming up the sample in 10 kOe magnetic field. (c) Temperature dependence of low field inverse magnetic susceptibility of MnSi. The paramagnetic Curie temperature (29 K) was determined through the extrapolation of data. (d) Temperature dependence of normalized magnetization of MnSi for 10 kOe magnetic field. The fitted line represents equation (1).

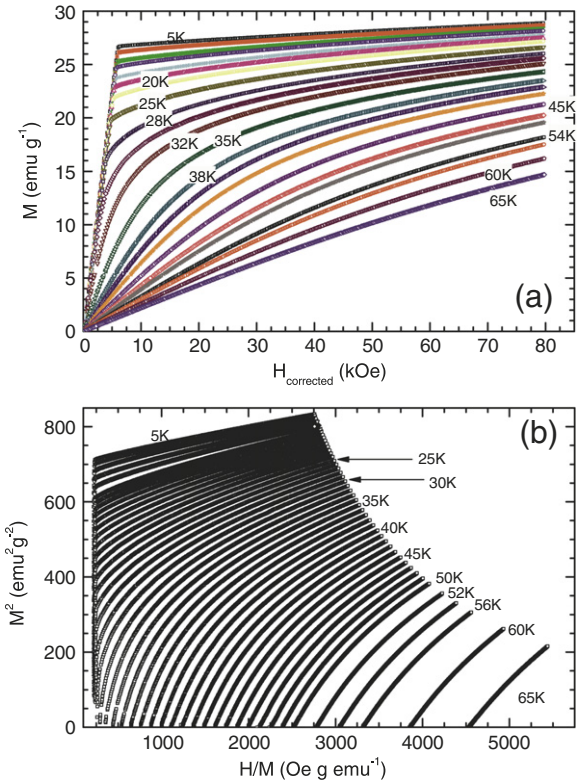

Figure 2. (a) Field dependence of isothermal magnetization of MnSi. The curves have been corrected for the demagnetizing fields. (b) The Arrott plots obtained from the (corrected) isothermal field dependence of magnetization of MnSi. The Arrott plots are nonlinear in nature.

fields, respectively. The temperature dependence of low field (100 Oe) magnetization shown in figure 1(a) is significantly different from that of a conventional ferromagnet and this has been discussed in our previous work [4]. However, the signature of a phase transition from the paramagnetic to an ordered magnetic state with decreasing temperature is clearly seen in both figures 1(a) and (b). The transition temperature determined from the inflection points in the M versus T curves in figures 1(a) and (b) is 31.5 K. Figure 1(c) shows the temperature dependence of the inverse magnetic susceptibility (χ^{-1}) of MnSi for $H = 100$ Oe. The paramagnetic Curie temperature of MnSi was determined by fitting a straight line (Curie–Weiss law) to the χ^{-1} versus T curve, which turns out to be 29 K.

Figure 1(d) shows the normalized magnetization of MnSi as a function of temperature for $H = 10$ kOe, from 2 to 50 K. The field 10 kOe is well above the field required for technical saturation of M in MnSi (see figure 2(a)). The $M(T)$ data were fitted with equation (1) given below:

$$\frac{M(T) - M(0)}{M(0)} = bT^{3/2} + cT^{5/2} + dT^2 + \cdots\cdots. \qquad (1)$$

Equation (1) fits the M versus T curve very well up to 26 K. The fitting of equation (1) gives useful information on the magnetic excitations present in MnSi. Here $M(0)$ is the magnetization at $T = 0$ for $H = 10$ kOe and is obtained by the extrapolation of the experimental $M(T)$ data. The $T^{3/2}$ term is due to excitations of long wavelength spin waves [16], the $T^{5/2}$ term results from spin wave–spin wave interactions [16] and the T^2 term arises from Stoner band excitations [17]. The magnitudes of b, c and d are found to be 32×10^{-5} K$^{-3/2}$, 4×10^{-5} K$^{-5/2}$ and 11×10^{-5} K^{-2}, respectively. The presence of the Stoner contribution suggests the significant role of itinerant electron ferromagnetism in MnSi. Similar T dependence of saturation magnetization has earlier been observed in other weak itinerant electron ferromagnetic systems, e.g. FeCoSi alloys [18], $ZrZn_2$, Ni_3Al, Fe–Ni invar alloys and NiPt alloys [19]. Here, it is worthwhile to mention that the spin wave excitation spectrum of MnSi has been investigated theoretically in the recent past [20]. In these investigations it was noted that there were a number of energy scales that are relevant to the magnetic behaviour of MnSi. These are: (i) the conventional isotropic exchange interaction that defines the in-plane ferromagnetic ordering, (ii) the (weak) Dzyaloshinski–Moriya interaction that produces the chirality of the spin structure and (iii) a few weaker terms like the anisotropic exchange interaction, the magnetic dipolar interaction and the Zeeman energy that affect the direction of the magnetic moment. The conventional isotropic exchange

interaction is the strongest among these energy scales and is relevant for $H = 10$ kOe. The other energy scales discussed above are relevant only at much lower field values. The use of equation (1) for the high field ferromagnetic state of MnSi is therefore justified in the present case.

On the basis of the Stoner model Wohlfarth *et al* have shown [19, 21, 22] that, for itinerant electron ferromagnets with homogeneous and weak magnetization, high field isothermal magnetization can be expressed as

$$M^2 = -\frac{A}{B} + \frac{1}{B}\left(\frac{H}{M}\right), \tag{2}$$

where A and B are independent of H. This should lead to linear and parallel M^2 versus H/M plots that are commonly referred to as Arrott plots [23]. Figure 2(a) depicts isothermal magnetization versus magnetic field curves (after correcting for demagnetizing fields [24]) of MnSi at various temperatures with a maximum applied field of 80 kOe. The Arrott plots obtained from the corrected $M(H)$ curves are shown in figure 2(b). The Arrott plots for MnSi are found to be nonlinear in nature, even at high fields. This is in sharp contrast to many itinerant electron ferromagnets including the isostructural helimagnetic FeCoSi system [18], $ZrZn_2$, Ni_3Al, Fe–Ni invar alloys and NiPt alloys [19]. Thus the $M(H)$ results on MnSi cannot be analysed using Wohlfarth's model, as has been done for other itinerant electron ferromagnetic systems [18, 19, 25–28]. This nonlinearity of the high field portions of the Arrott plots of MnSi was earlier pointed out by Bloch *et al* [29] but detailed investigation of this behaviour, to the best of our knowledge, has not been carried out so far. The results of such an investigation are presented below.

The Arrott plots are based on a power series expansion of the Brillouin function obtained using the molecular field approximation [30]. Extrapolation of the high field part (to avoid the regime where domain alignment is not complete [30]) of Arrott plots to $H/M = 0$ and $M^2 = 0$, respectively, gives M_s^2 (for $T < T_C$) and the inverse initial susceptibility χ^{-1} (for $T > T_C$). When the high field parts of the Arrott plots are nonlinear, extrapolating the curves becomes difficult. In such cases the proper critical exponents for the system have to be determined and the experimental data must be fitted to the equation of state [23]:

$$\left(\frac{H}{M}\right)^{1/\gamma} = \frac{T - T_C}{T_1} + \left(\frac{M}{M_1}\right)^{1/\beta}. \tag{3}$$

Here, T_1 and M_1 are material-dependent constants; β and γ are the critical exponents that define the temperature dependence of M_s and χ^{-1} close to T_C in the following way:

$$\begin{aligned} M_s &\propto \left(1 - \frac{T}{T_C}\right)^{\beta}, \qquad T < T_C \\ \chi^{-1} &\propto \left(\frac{T}{T_C} - 1\right)^{\gamma}, \qquad T > T_C. \end{aligned} \tag{4}$$

If β and γ are determined correctly, the isothermal $M^{1/\beta}$ versus $(H/M)^{1/\gamma}$ plots near T_C should produce a set of parallel straight lines [30]. The T_C could be easily determined from such plots.

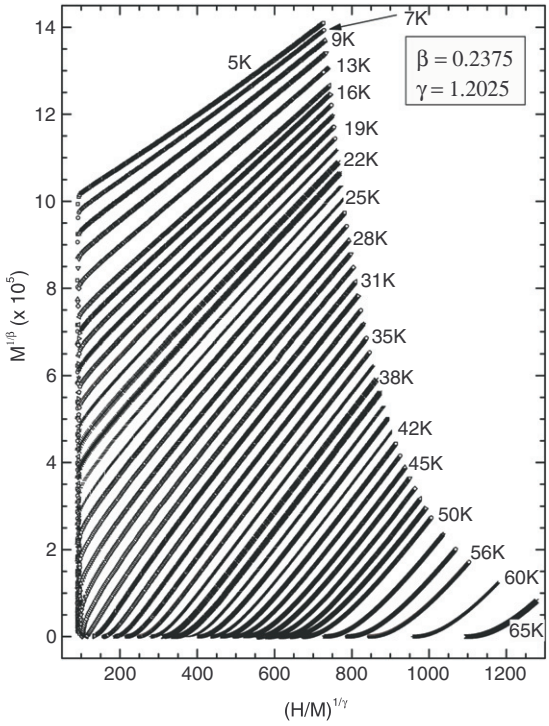

Figure 3. The modified Arrott plots for MnSi obtained using the iterative technique (see the text for details).

We shall now carry out the process of linearizing the Arrott plots in MnSi. However, we note here that we are actually dealing with the field-induced ferromagnetic state of MnSi and we recall that the zero-field magnetic state is helimagnetic in nature. So the critical exponent we will be dealing with here is not that of the zero-field helimagnetic state, but that of the hypothetical magnetic state in the zero-field limit of the field-induced ferromagnetic state of MnSi. With this assumption the β and γ values for MnSi were calculated using Kaul's method [31] and were refined further using the Kouvel–Fisher method [32]. This was done in the following way. Approximate values of M_s were determined from the M^2 versus H/M plots (figure 2(b)) and the temperature dependence of M_s was used to find the trial value [31] of β (=0.3087). The trial value of γ (= 1.8121) was obtained from low field (100 Oe) M versus T results shown in figure 1(a). Using these trial values, $M^{1/\beta}$ versus $(H/M)^{1/\gamma}$ plots were obtained. By extrapolating the high field parts of these plots to $(H/M)^{1/\gamma} = 0$ and $M^{1/\beta} = 0$, respectively, new values of M_s (for $T < T_C$) and χ^{-1} (for $T > T_C$) were obtained. The β and γ values were then calculated again using equation (4) and were further corrected using the Kouvel–Fisher method [32]. The T_C was also determined using the Kouvel–Fisher method [32]. The whole procedure was iterated six times (until the values of β, γ and T_C converged with those of the previous iteration) to get the final values of β, γ and T_C, respectively, as 0.2375, 1.2025 and 29.67 K. The $M^{1/\beta}$ versus $(H/M)^{1/\gamma}$ plots obtained with these values of β and γ are shown in figure 3. These modified Arrott plots are quite

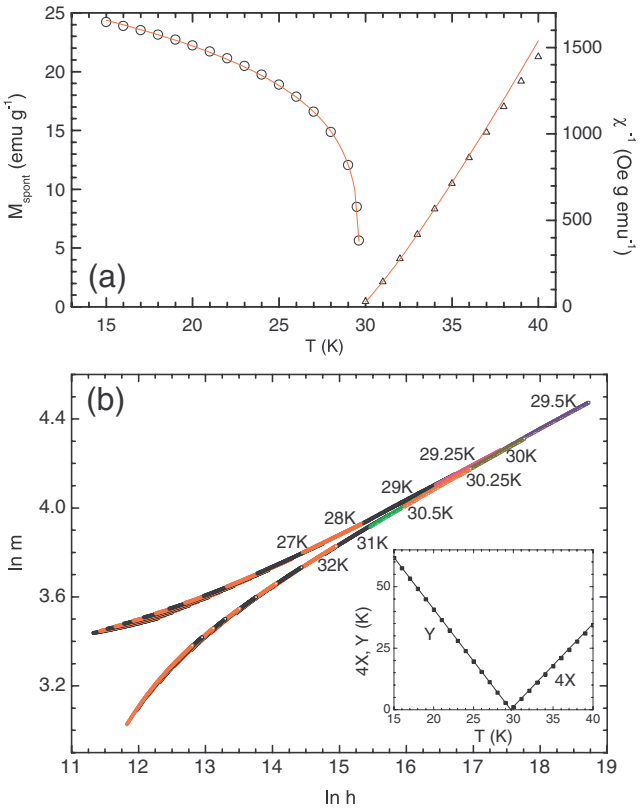

Figure 4. (a) Temperature dependence of spontaneous magnetization (open circles) and high temperature inverse magnetic susceptibility (open triangles) for MnSi. The fitted lines represent equation (4). (b) Log of reduced magnetization versus log of reduced field (see the text for details) confirming the correctness of the obtained values of the critical exponents and the transition temperature. Inset to (b): Kouvel–Fisher plot (see the text for details) confirming the correctness of the T_C.

linear in nature. The temperature dependences of M_s and χ^{-1} are shown in figure 4(a). This figure depicts the data between 15 and 40 K to highlight the region close to T_C. The theory of critical exponents is applicable only in the region close to T_C [24, 30–32], and in the present case the χ^{-1} versus T data above 40 K could not be fitted very well with equation (4). The critical exponent δ was determined using the Widom scaling relation $\gamma = \beta(\delta - 1)$ [24, 30]. In this method δ comes out to be 6.06.

The β, γ and T_C values estimated in the procedure mentioned above are further cross-checked using the scaling hypothesis laid down by Griffiths [33]. A simpler form of these scaling equations evolved due to the efforts of Stanley *et al* [34] and Kouvel *et al* [35]. It follows that, if β, γ and T_C are correctly determined, then in the $\ln(M/|1 - T/T_C|^{\beta})$ versus $\ln(H/|1 - T/T_C|^{\beta+\gamma})$ plots all the isothermal M versus H data near T_C fall on two universal curves separated from each other at T_C. This is clearly seen in figure 4(b), where the two curves separate out from each other between 29.5 and 30 K. The correctness of the T_C is also confirmed from the Kouvel–Fisher plot [31, 32] shown in the inset to figure 4(b). In this inset, X and Y are defined as $X = \chi^{-1}(\frac{\partial \chi^{-1}}{\partial T})^{-1} = \frac{T-T_C}{\gamma}$ and $Y = -M_s(\frac{\partial M_s}{\partial T})^{-1} = -\frac{T-T_C}{\beta}$, and X has been multiplied by 4 to plot X and Y on the same scale.

We now estimate the errors in β, γ, δ and T_C determined above. All these physical quantities are obtained from isothermal M versus H results for magnetic fields from 30 to 80 kOe. During the measurement of magnetization of MnSi in the VSM used for the present work, the error in M is less than 10^{-4}%. The error in the value of H during such a measurement typically varies from 0.01% to 0.1%. The error in temperature during the isothermal magnetization measurements is less than 0.1%. The errors in β, γ and T_C incorporated by the curve fitting procedure are respectively 0.4%, 1% and 0.3%. Combining all these errors it is found that the value of β (=0.2375) would have a maximum error of $\pm$0.0014. The γ value (=1.2025) would contain a maximum error of $\pm$0.0144. Since δ is determined from the Widom scaling relation, the maximum proportionate error in δ is obtained by combining the errors in β and γ. Thus the maximum error in the value of δ (=6.06) is $\pm$0.109.

Apart from using the Widom scaling relation $\gamma = \beta(\delta - 1)$, the critical exponent δ is also determined from the M versus H curves using the power law $M \propto H^{1/\delta}, T \approx T_C$ [24, 30]. In this method, the δ for MnSi comes out to be approximately 6.25. Although this value appears quite close to that obtained from the Widom scaling relation, the difference between the two values is actually larger than the error involved in the determination of δ (see the error calculation above). This difference is presumably caused by the low field phase transitions occurring in MnSi (described in section 1). For the determination of the critical exponents β and γ, only the high field (greater than 30 kOe) parts of the modified (linear) Arrott plots were extrapolated. Thus the presence of the field-induced phase transitions did not affect the determination of β and γ (and hence δ, when determined from the Widom scaling relation). However, for the determination of δ from the power law, the M versus H curves are used directly [31, 32]. Hence this value of δ is likely to be affected by the lower field transitions. The values of β and γ determined in the above method do not match with those obtained from the Heisenberg and Ising models [31, 36, 37]. On the other hand, the values of β (0.2375) and γ (1.2025) determined here for MnSi are quite similar to those reported for the metallic ferromagnet CoS_2 [38] and helimagnetic systems β-MnO_2 and $CsMnBr_3$ [39]. We also observe that the values of β and γ in MnSi are quite close to those calculated for the helimagnetic systems [40, 41]. The actual zero-field state of MnSi being helimagnetic [1], this latter finding may not just be a coincidence.

The method of Arrott plots described above has been used extensively to find the critical exponents and T_C of different ferromagnetic systems including single crystals, thin film multilayers, polycrystalline materials, liquid ferromagnets and organic ferromagnets [31, 36, 37, 42]. The method is not necessarily restricted to single crystals. We therefore believe that the gross physical outcome of the present analysis will not change if the same analysis is performed on a single crystal of MnSi. Also, in this analysis it is assumed that the magnetic phase transition at the determined T_C is of second-order nature. This assumption is based on previous work [13, 43] where the ordering temperature of MnSi is taken to be a combination of

a lower temperature first-order phase transition and a higher temperature second-order phase transition.

4. Summary and conclusion

The temperature dependence of the saturation magnetization of MnSi exhibits the signatures of both spin wave excitations and Stoner band excitations related to itinerant electron ferromagnetism. However, the standard Arrott plots for MnSi are highly nonlinear and hence the ferromagnetic character of the field-induced state in MnSi cannot be analysed in a straightforward manner within the framework of itinerant electron magnetism [19, 21, 22]. The modified Arrott plots for MnSi are found to be linear, and the critical exponents of the field-induced ferromagnetic state of MnSi in its zero-field limit were determined using the high field portions of the Arrott plots. The values of the critical exponents are found to be quite close to another metallic ferromagnetic system (CoS_2). Interestingly, the reported values of the critical exponents for the helimagnetic systems are also found to be close to those obtained for MnSi.

References

[1] Ishikawa Y, Tajima K, Bloch D and Roth M 1976 *Solid State Commun.* **19** 525
[2] Williams H J, Wernick J H, Sherwood R C and Wertheim G K 1966 *J. Appl. Phys.* **37** 1256
[3] Koyama K, Goto T, Kanomata T and Note R 2000 *Phys. Rev.* B **62** 986
[4] Roy S B and Chattopadhyay M K 2007 *Europhys. Lett.* **79** 47007
[5] Thompson J D, Fisk Z and Lonzarich G G 1989 *Physica* B **161** 317
[6] Uemura Y J, Goko T, Gat-Malureanu I M, Carlo J P, Russo P L, Savici A T, Aczel A, MacDougall G J, Rodriguez J A, Luke G M, Dunsiger S R, McCollam A, Arai J, Pfleiderer C, Böni P, Yoshimura K, Baggio-Saitovitch E, Fontes M B, Larrea J, Sushko Y V and Sereni J 2007 *Nat. Phys.* **3** 29
[7] Pfleiderer C, Böni P, Keller T, Rößler U K and Rosch A 2007 *Science* **316** 1871
[8] Petrova A E, Krasnorussky V, Sarrao J and Stishov S M 2006 *Phys. Rev.* B **73** 052409 and references therein
[9] Petrova A E, Bauer E D, Krasnorussky V and Stishov S M 2006 *Phys. Rev.* B **74** 092401
[10] Matsunaga M, Ishikawa Y and Nakajima T 1982 *J. Phys. Soc. Japan* **51** 1153
[11] Pfleiderer C 2001 *J. Magn. Magn. Mater.* **226** 23
[12] Rößler U K, Bogdanov A N and Pfleiderer C 2006 *Nature* **442** 797
[13] Stishov S M, Petrova A E, Khasanov S, Panova G K, Shikov A A, Lashley J C, Wu D and Lograsso T A 2007 *Phys. Rev.* B **76** 052405
[14] Stishov S M, Petrova A E, Khasanov S, Panova G K, Shikov A A, Lashley J C, Wu D and Lograsso T A 2007 arXiv:cond-mat/0702460v1
[15] Arora P, Chattopadhyay M K and Roy S B 2007 *Appl. Phys. Lett.* **91** 062508
[16] Argyle B E, Charap S H and Pugh E W 1963 *Phys. Rev.* **132** 2051
[17] Chien C L and Hasegawa R 1977 *Phys. Rev.* B **16** 2115
[18] Chattopadhyay M K, Roy S B, Chaudhary S, Singh K J and Nigam A K 2002 *Phys. Rev.* B **66** 174421
[19] Wohlfarth E P 1977 *Physica* B **91** 305 and references therein
[20] Maleyev S V 2006 *Phys. Rev.* B **73** 174402
Kirkpatrick T R and Belitz D 2005 *Phys. Rev.* B **72** 180402(R)
Belitz D, Kirkpatrick T R and Rosch A 2006 *Phys. Rev.* B **73** 054431
[21] Edwards D M and Wohlfarth E P 1968 *Proc. R. Soc.* A **303** 127
[22] Wohlfarth E P 1968 *J. Appl. Phys.* **39** 1061
[23] Arrott A and Noakes J E 1967 *Phys. Rev. Lett.* **19** 786
[24] Blundell S 2006 *Magnetism in Condensed Matter* (New York: Oxford University Press)
[25] Yamada O, Ono F and Nakai I 1977 *Physica* B **91** 298
Mills D L 1971 *Solid State Commun.* **9** 929
[26] Brommer P E and Franse J J M 1996 *Ferromagnetic Materials* vol 5, ed K H J Bushow and E P Wohlfarth (New York: Elsevier Science) p 323
[27] Alberts H L, Beille J, Bloch D and Wohlfarth E P 1974 *Phys. Rev.* B **9** 2233
[28] Abu-Aljarayesh I and Said M R 2000 *J. Magn. Magn. Mater.* **210** 73
[29] Bloch D, Voiron J, Jaccarino V and Wernick J H 1975 *Phys. Lett.* A **51** 259
[30] Aharoni A 1996 *Introduction to the Theory of Ferromagnetism* (New York: Oxford University Press)
[31] Kaul S N 1985 *J. Magn. Magn. Mater.* **53** 5
[32] Kouvel J S and Fisher M E 1964 *Phys. Rev.* **136** A1626
[33] Griffiths R B 1967 *Phys. Rev.* **158** 176
[34] Milosevic S and Stanley H E 1972 *Phys. Rev.* B **5** 2526
Milosevic S and Stanley H E 1972 *Phys. Rev.* B **6** 986
Milosevic S and Stanley H E 1972 *Phys. Rev.* B **6** 1002
[35] Kouvel J S and Comly J B 1968 *Phys. Rev. Lett.* **20** 1237
Kouvel J S and Rodbell D S 1967 *Phys. Rev. Lett.* **18** 215
[36] Seeger M, Kaul S N, Kronmüller H and Reisser R 1995 *Phys. Rev.* B **51** 12585
Yang F Y, Chien C L, Li X W, Xiao G and Gupta A 2001 *Phys. Rev.* B **63** 092403
Yanagihara H, Cheong W, Salamon M B, Xu S and Morimoto Y 2002 *Phys. Rev.* B **65** 092411
[37] Mohan C V and Kornmüller H 1998 *J. Magn. Magn. Mater.* **182** 287 and references therein
[38] Hiraka H and Endoh Y 1994 *J. Phys. Soc. Japan* **63** 4573
[39] Sato H, Kawamura Y, Ogawa T, Murakami Y, Oshumi H, Mizumaki M and Ikeda N 2003 *Physica* B **329–333** 757
Plakhty V P, Kulda J, Visser D, Moskvin E V and Wosnitza J 2000 *Phys. Rev. Lett.* **85** 3942
[40] Kawamura H 1988 *J. Appl. Phys.* **63** 3086
[41] Plumer M L and Mailhot A 1994 *Phys. Rev.* B **50** 16113
[42] Tsurkan V, Baran M, Szewezyk A, Szymezak R and Szymezak H 1999 *J. Phys.: Condens. Matter* **11** 7907
Bührer C, Beckmann M, Fähnle M, Grünewald U and Maier K 2000 *J. Magn. Magn. Mater.* **212** 211
Coelho A A, Mohan C V, Gama S and Kornmüller H 1996 *J. Magn. Magn. Mater.* **163** 87
Mohan C V, Seeger M, Kornmüller H, Murugaraj P and Maier J 1998 *J. Magn. Magn. Mater.* **183** 348
Girtu M A, Wynn C M, Zhang J, Miller J S and Epstein A J 2000 *Phys. Rev.* B **61** 492
[43] Stishov S M, Petrova A E, Khasanov S, Panova G K, Shikov A A, Lashley J C, Wu D and Lograsso T A 2008 *J. Phys.: Condens. Matter* **20** 235222